Conceptual Design and Challenges for Drift Chambers

The path to a drift chamber design and the plans to overcome the challenges

F. Grancagnolo

INFN – Lecce

ECFA WG3: Topical workshop on tracking and vertexing

CERN, 30–31 May 2023

Tracking requirements

- Large **angular coverage**
- High **angular resolution** ($\Delta\vartheta \leq 0.1$ mrad for monitoring beam spread ($Z \rightarrow \mu\mu$))
- High **granularity** (to cope with occupancy at inner radii)
- High **tracking efficiency**
- High **momentum resolution**
  $\delta p/p^2 \leq$ few x 10^{-5}, small wrt 0.12% beam spread for
  - Higgs mass recoil
  - cLFV processes like $Z \rightarrow e\mu$,$e\tau$, $\mu\tau$ (BR $\approx 10^{-54} - 10^{-60}$)
    current exp. limits ($\leq 10^{-6}$) can be improved by > 5 orders of magnitude
- High capabilities for **Particle Identification** (dE/dx resolutions $\lesssim 3\%$)
  - Flavor Physics
  - CPV ($B_s \rightarrow D_s K$)
  - A_{FB}(b), exclusive b-hadron decays reconstruction
  - Hadron spectroscopy
- High **V^0 and kink** capability for CPV (CP eigenstates usually long-lived particles)

Physics requirements: momentum

$$\sigma_{p_T}/p_T^2 \approx 2\times10^{-5}\ (\text{GeV/c})^{-1}$$

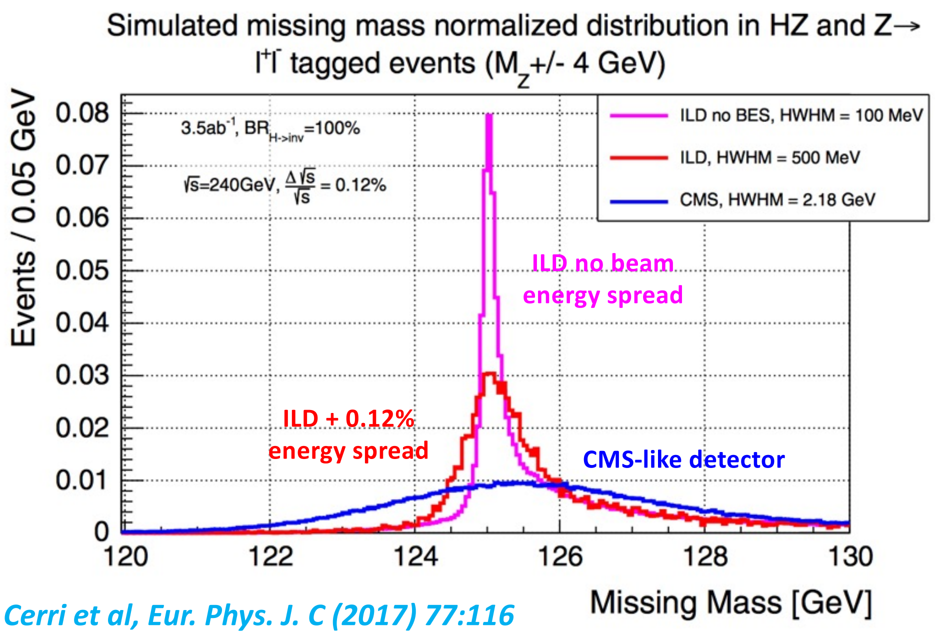

Cerri et al, Eur. Phys. J. C (2017) 77:116

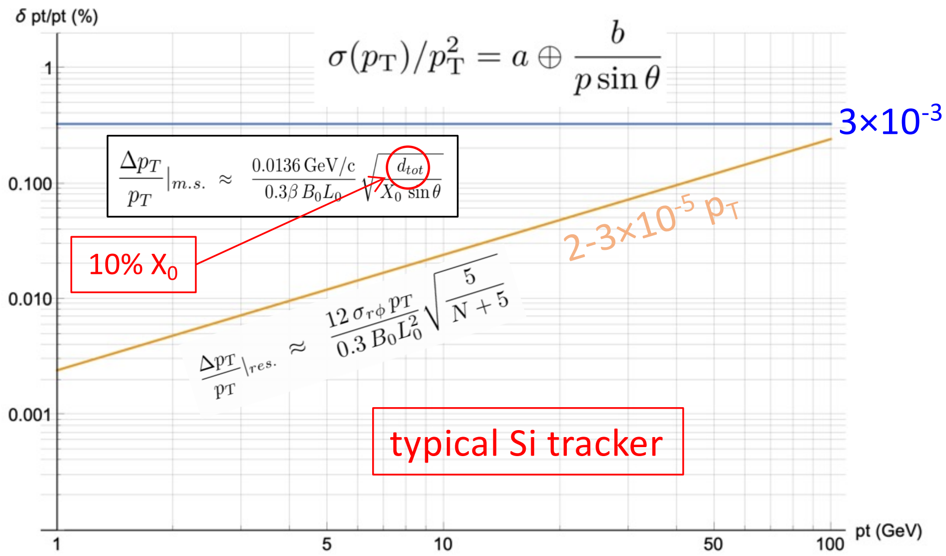

Drasal, Riegler, https://doi.org/10.1016/j.nima.2018.08.078

Physics requirements: PID

Example: $B_s^0 \to D_s^{\mp} K^{\pm}$

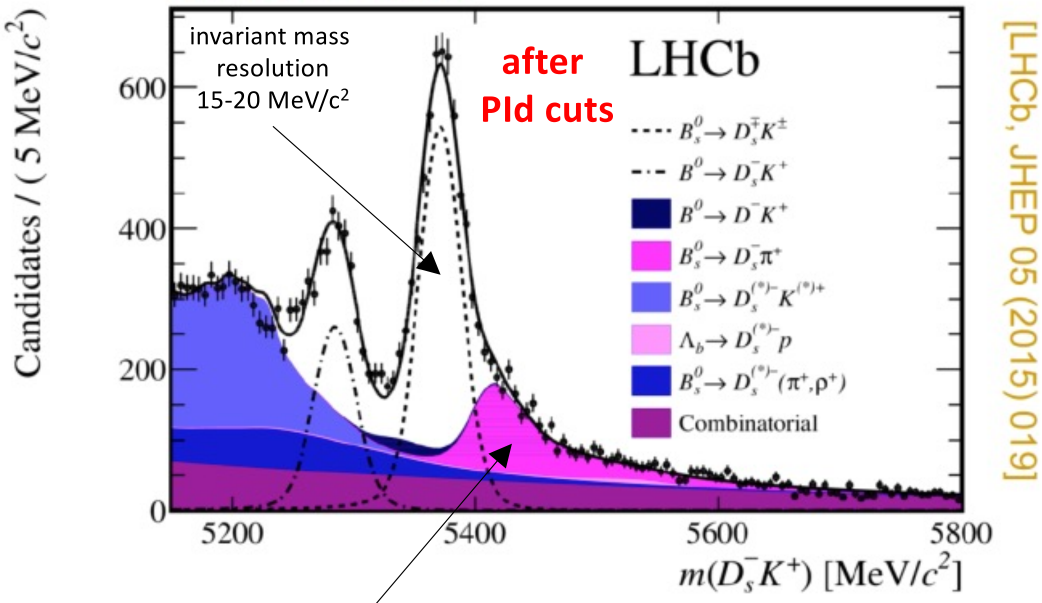

$B_s^0 \to D_s^- \pi^+$
contribution reduced by a factor x10
(60% efficiency – 1% contamination)

R. Aleksan , L. Oliver and E. Perez - arXiv:2107.02002v1 [hep-ph] 5 Jul 2021

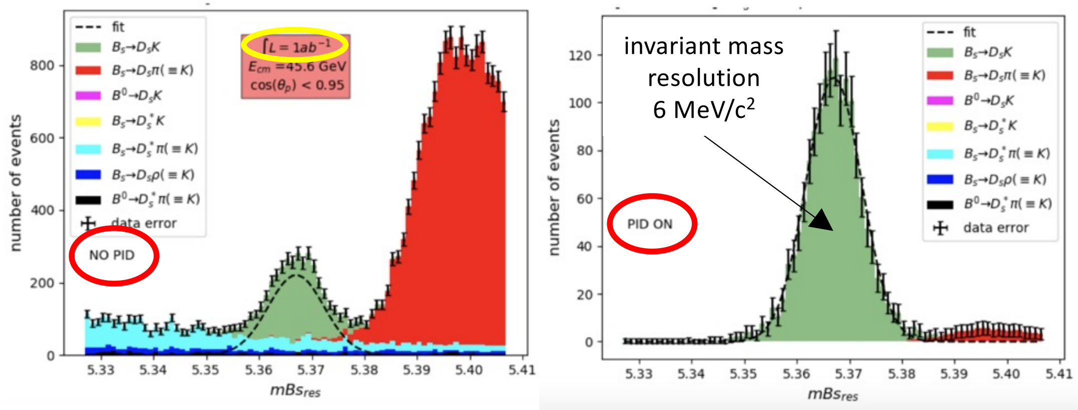

PID at 5% and TOF at 100 ps

Range of momenta

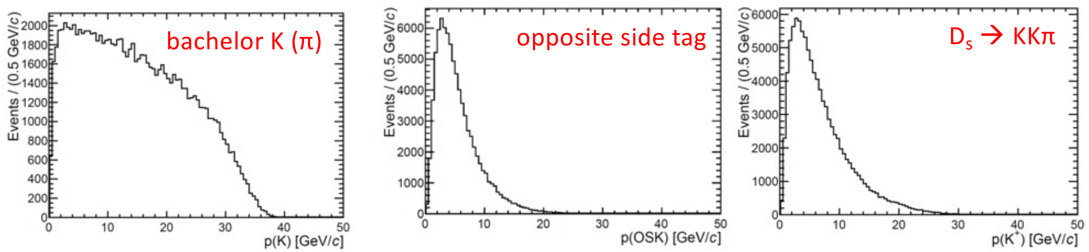

Guy Wilkinson - Particle identification at FCC-ee - Eur. Phys. J. Plus (2021) 136:835 – https://doi.org/10.1140/epjp/s13360-021-01810-4

Why a Drift Chamber?

Trackers at e^+e^- Colliders

past

SPEAR	MARK2	Drift Chamber
	MARK3	Drift Chamber
DORIS	PLUTO	MWPC
	ARGUS	Drift Chamber
CESR	CLEO1,2,3	Drift Chamber
VEPP2/4M	CMD-2	Drift Chamber
	KEDR	Drift Chamber
	NSD	Drift Chamber
PETRA	CELLO	MWPC + Drift Ch.
	JADE	Drift Chamber
	PLUTO	MWPC
	MARK-J	TEC + Drift Ch.
	TASSO	MWPC + Drift Ch.
TRISTAN	AMY	Drift Chamber
	VENUS	Drift Chamber
	TOPAZ	TPC

PEP	MARK2	Drift Chamber
	PEP-4	TPC
	MAC	Drift Chamber
	HRS	Drift Chamber
	DELCO	MWPC
BEPC	BES1,2	Drift Chamber
LEP	ALEPH	TPC
	DELPHI	TPC
	L3	Si + TEC
	OPAL	Drift Chamber
SLC	MARK2	Drift Chamber
	SLD	Drift Chamber
DAPHNE	KLOE	Drift Chamber
PEP2	BaBar	Drift Chamber
KEKB	Belle	Drift Chamber

present

VEPP2000	CMD-3	Drift Chamber
	KEDR	Drift Chamber
BEPC2	BES3	Drift Chamber
S.KEKB	Belle2	Drift Chamber

future

ILC	ILD	TPC	
	SiD	Si	
CLIC	CLIC	Si	
FCC-ee	CLD	Si	
	IDEA	Drift Chamber	
CEPC	Baseline	TPC	Si
	4th	Si + Drift Chamber	
	IDEA	Drift Chamber	
SCTF	BINP	Drift Chamber	
STCF	HIEPA	Drift Chamber	

Evolution of momentum resolution

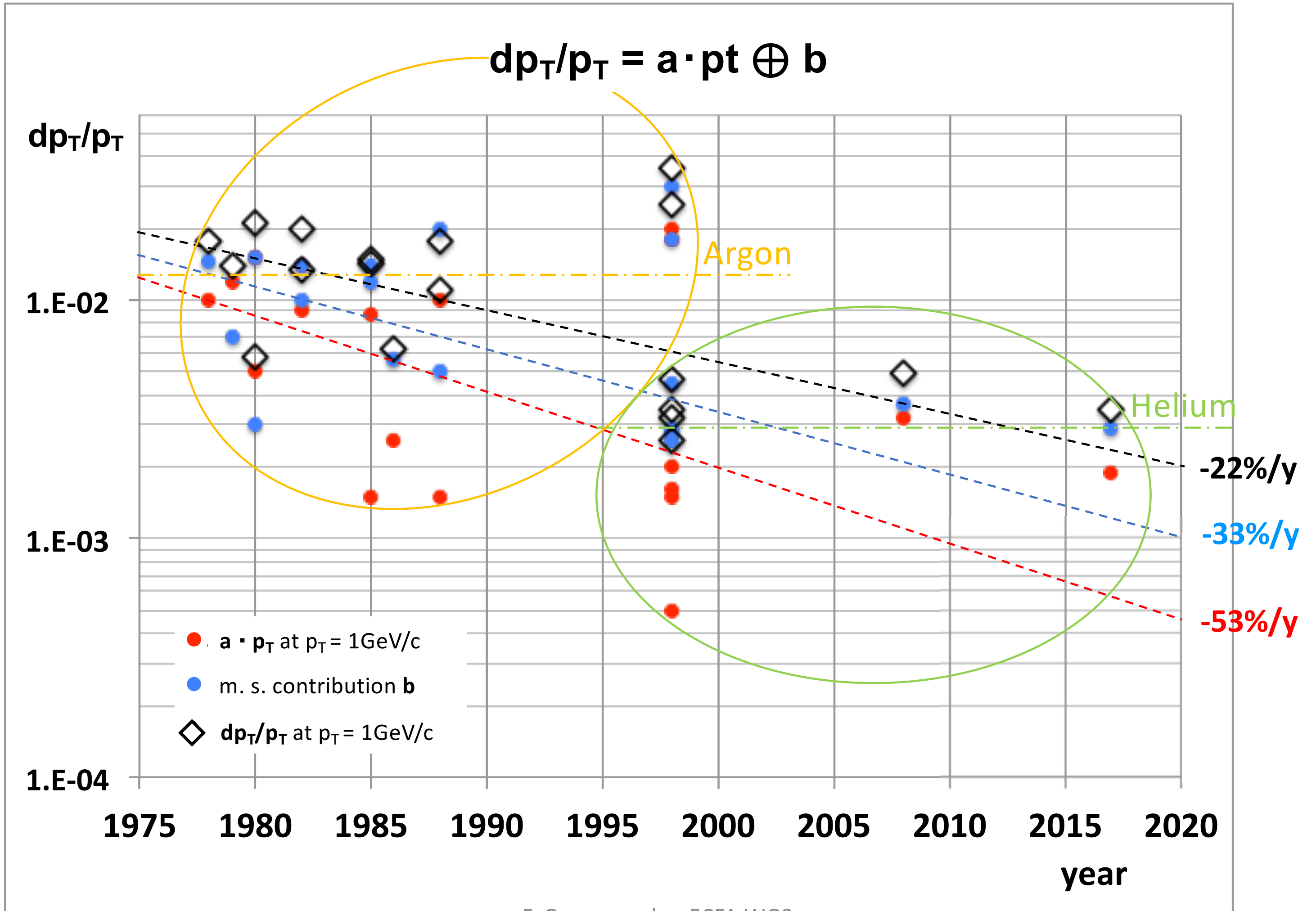

The path to a conceptual design and the challenges

Design

- Geometrical acceptance
- Momentum and angle resolution
- Occupancy and cell size
- Layer structure
- Material budget
  - Layer structure
  - Cell structure
  - Gas mixture
- Mechanical structure
- Particle Identification
  - cluster counting constraints
  - cluster timing benefits
- Overall performance

Challenges

- Mechanics
  - types of wires
  - number of wires
  - gas envelope
  - wire cage
  - material choice
- Simulations: dN/dx and dE/dx
- Electronics
  - front end bandwidth
  - digitization
  - data reduction
  - data acquisition

Momentum and Angular Resolutions

$$\frac{\Delta p_T}{p_T}\Big|_{res.} = \frac{\sigma_{r\phi}\, p_T}{0.3\, B_0 L_0^2}\sqrt{\frac{720N^3}{(N-1)(N+1)(N+2)(N+3)}}$$

$$\approx \frac{12\,\sigma_{r\phi}\, p_T}{0.3\, B_0 L_0^2}\sqrt{\frac{5}{N+5}}$$

$$\frac{\Delta p_T}{p_T}\Big|_{m.s.} = \frac{N}{\sqrt{(N+1)(N-1)}}\,\frac{0.0136\,\mathrm{GeV/c}}{0.3\beta\, B_0 L_0} \times \sqrt{\frac{d_{tot}}{X_0\,\sin\theta}}\left(1+0.038\ln\frac{d}{X_0\,\sin\theta}\right)$$

$$\approx \frac{0.0136\,\mathrm{GeV/c}}{0.3\beta\, B_0 L_0}\sqrt{\frac{d_{tot}}{X_0\,\sin\theta}}$$

$$\Delta\theta|_{res.} = \frac{\sigma_z\,\sin^2\theta}{L_0}\sqrt{\frac{12N}{(N+1)(N+2)}}$$

$$\approx \frac{2\,\sigma_z\,\sin^2\theta}{L_0}\sqrt{\frac{3}{N+3}}$$

$$\Delta\theta|_{m.s.} = \frac{\sin\theta}{\beta\, p_T}\, f\left(\frac{d}{X_0\,\sin\theta}\right)$$

$$\approx \frac{0.0136\,\mathrm{GeV/c}\,\sin\theta}{\beta\, p_T}\sqrt{\frac{d}{X_0\,\sin\theta}}$$

$$\Delta\phi|_{res.} \approx \frac{\sigma_{r\phi}}{L_0}\,\frac{8\sqrt{3}}{\sqrt{N+5}}\sqrt{1+\frac{15}{4}\frac{r_0}{L_0}+\frac{15}{4}\frac{r_0^2}{L_0^2}}$$

$$\Delta\phi|_{m.s.} \approx \frac{0.0136\,\mathrm{GeV/c}}{\beta p_T}\sqrt{\frac{d}{X_0\sin\theta}}\sqrt{1+2\left(\frac{r_0}{L_0}\right)+4\left(\frac{r_0}{L_0}\right)^2}$$

An extension of the Gluckstern formulae for multiple scattering: Analytic expressions for track parameter resolution using optimum weights

Z. Drasal[a,b], W. Riegler[b,*] https://doi.org/10.1016/j.nima.2018.08.078

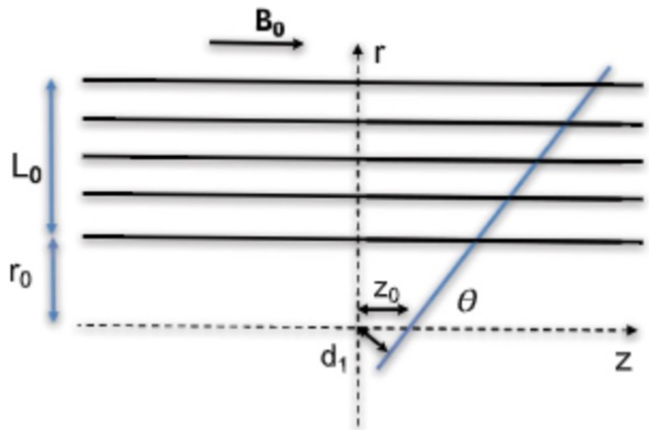

Acceptance constraints:

$\Delta\Omega \approx 98.5\% \implies \vartheta_{min} = 10°$

$r_0 = L_z/2 \tan\vartheta_{min} = 0.35$ m

(also considerations about **occupancy** due to **beam bkgnds**)

given **B_0 = 2 Tesla**, **L_0 = 1.65 m**, at high momenta:

$\Delta(1/p_T) \sim \mathbf{2\times10^{-5}} \implies N > 100,\ \sigma_{r\phi} \lesssim 100\ \mu m$ $\quad$ (*for a drift chamber, DC*)

$\implies N > 5,\ \sigma_{r\phi} \lesssim 30\ \mu m$ $\quad$ (*for a solid state detector, SSD*)

at low (multiple scattering dominated) momenta:

$\Delta(1/p_T) \sim \mathbf{1\times10^{-3}/(p_T \cdot \sin\vartheta)} \implies d_{tot} \lesssim 5\times10^{-3}X_0$ $\quad$ (*~ satisfied for a DC, gas + wires*)

(*≅ one single plane of a SSD*)

with **r_0 = 0.35 m**, **ϑ = 45°**, **p = 45 GeV/c** (p_T = 32 GeV/c):

$\Delta\vartheta|_{m.s.}$ and $\Delta\phi|_{m.s.}$ ≈ 40 μrad

Occupancy and drift cell size

Background studies for CDR

Background	Average occupancy $\sqrt{s}$ = 91.2 GeV	Average occupancy $\sqrt{s}$ = 365 GeV
e^+e^- pair background	1.1%	2.9%
$\gamma\gamma \to$ hadrons	0.001%	0.035%
Synchrotron radiation	negligible	0.2%

IPC dominant

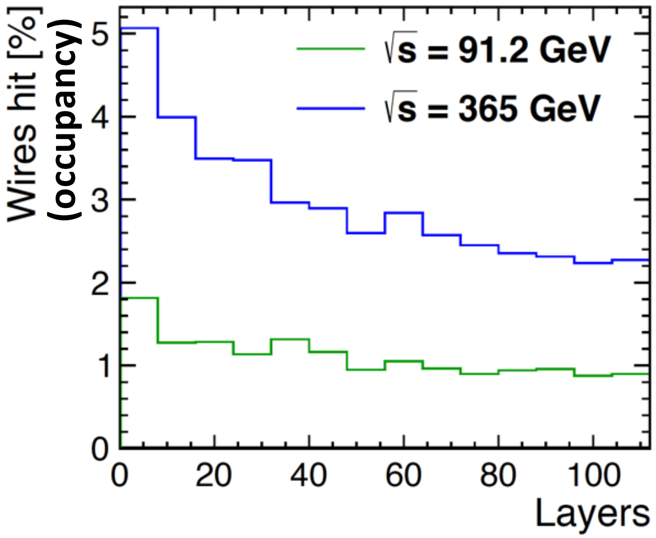

< 2% **occupancy** on first superlayer, < 5% on first layer, ≲10 spurious hits at r = 35 cm and drift cell = 1.2 cm))

Electrostatic stability condition

$$T_c \geq \frac{C^2 V_0^2}{4\pi\epsilon w^2} L^2$$

T_c wire tension
w cell width
L wire length

C capacitance per unit length
V_0 voltage anode-cathode

For w = 1 cm, L = 4 m:

T_c > 26 g for 40 μm Al field wires (δ_{grav} = 260 μm)
T_c > 21 g for 20 μm W sense wires (δ_{grav} = 580 μm)

Elastic limit condition

T_c < YTS × π ·r_w^2 *YTS = 750 Mpa* for W, *290 Mpa for Al*
T_c < 36 g for 40 μm Al field wires (δ_{grav} = 190 μm)
T_c < 24 g for 20 μm W sense wires (δ_{grav} = 510 μm)

The drift chamber length (**L = 4 m**) imposes strong constraints on the drift cell size (**w = 1 cm**)
Very little margin left ⇒ increase wires radii or cell size
⇒ use different types of wires

Geometry: layer structure

So far :

Geometrical acceptance	⇨	R_{in} = 0.35 m, R_{out} = 2.0 m, L = 4.0 m
Transverse momentum resolution	⇨	B_0 = 2 T, N > 100, $\sigma_{r\phi} \approx 100\ \mu m$,
Multiple scattering contribution	⇨	$d_{tot} \lesssim 5\times10^{-3}\ X_0$ (inner wall + gas + wires)
Occupancy and cell size	⇨	w ≈ 1.2 cm, L/w ≲ 400

Angular resolution:

$\Delta\vartheta = \Delta\vartheta|_{res.} \oplus \Delta\vartheta|_{m.s.} \lesssim 70\ \mu rad$,

(for monitoring beam energy spread at Z-pole at ϑ = 45°, p = 45 GeV/c

⇩

$\Delta\vartheta|_{res.} \lesssim 60\ \mu rad \implies$ **N > 100** and **$\sigma_z \lesssim 0.6$ mm**

$\implies$ **all layers stereo** at an angle **<±ε> ≳ 150 mrad**

($\tan\varepsilon \gtrsim \sigma_{r\phi}/\sigma_z$)

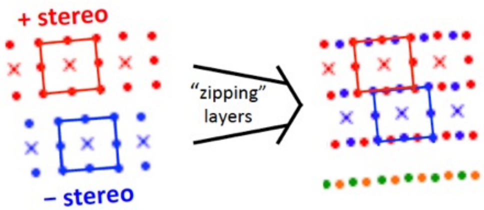

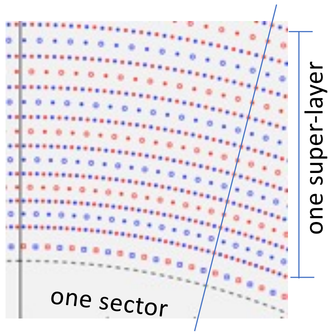

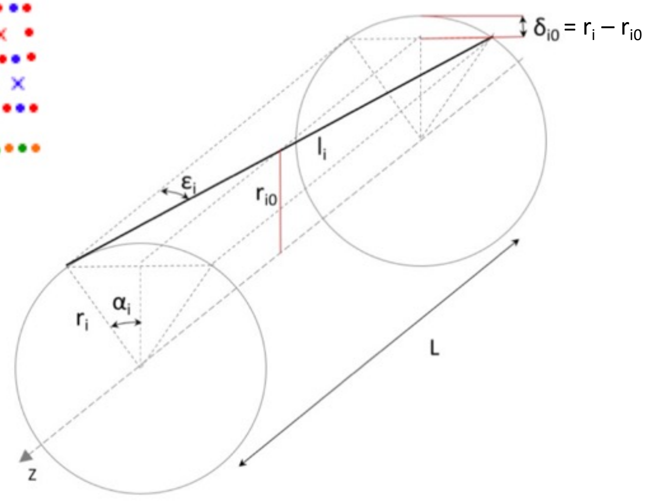

Drift Chamber geometry layout and material budget

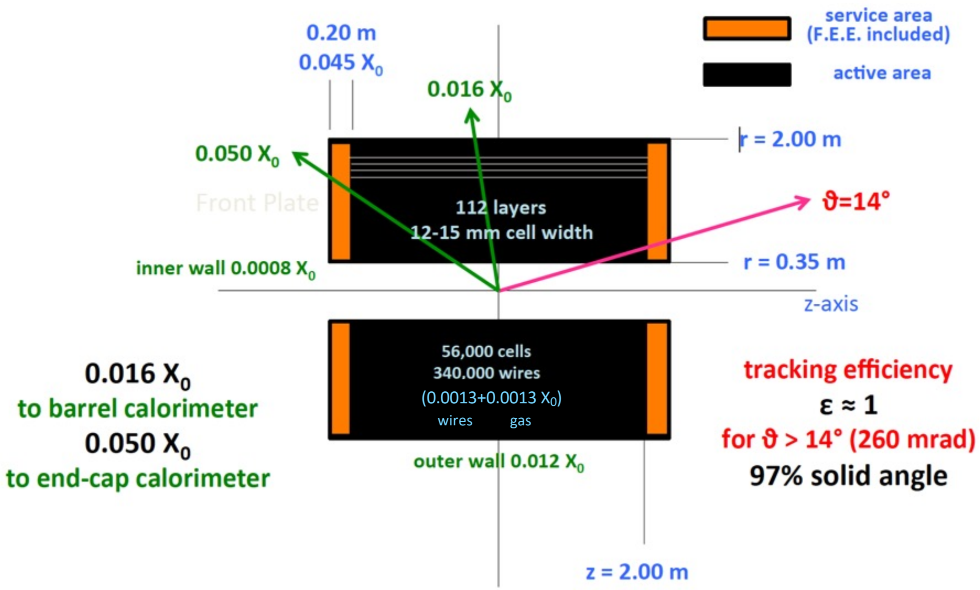

12 to 15 mm wide square cells, 5:1 field to sense wires ratio: 56,448 cells - 342,720 wires

14 co-axial super-layers, 8 layers each (112 total) with alternating sign stereo angles ranging from 50 to 250 mrad, in 24 equal azimuthal (15°) sectors

Material budget estimates

- Inner wall (from CMD3 drift chamber) — **8.4×10^{-4} X_0**
  - 200 μm Carbon fiber
- Gas (from KLOE drift chamber) — **1.3×10^{-3} X_0**
  - 90% He – 10% iC_4H_{10}
- Wires (from MEG2 drift chamber) — **1.3×10^{-3} X_0**
  - 20 μm W sense wires 6.8×10^{-4} X_0
  - 40 μm Al field wires 4.3×10^{-4} X_0
  - 50 μm Al guard wires 1.6×10^{-4} X_0
- Outer wall (from Mu2e I-tracker studies) — **1.2×10^{-2} X_0**
  - 2 cm composite sandwich (7.7 Tons)
- End-plates (from Mu2e I-tracker studies) — **4.5×10^{-2} X_0**
  - wire cage + gas envelope
  - incl. services (electronics, cables, ...)

Increase cell size to *w > 1.5 cm (+10%)*

(56,448 → 45,700 cells, 112 → 100 layers, 340,000 → 500,000 wires, 9 → 18 Ton)

and **replace 20 μm W and 40-50 μm Al** (5:1) with

(2 (0.5) μm Ag coated) **35 μm C wires** (10:1). Stability condition:

30 g < T_c < 87 g corresponding to ***270 (158) μm > δ_{grav} > 93 (54) μm***

(safety factor within ample margin!)

Contribution to m. scatt. from wires: 1.3×10^{-3} X_0 → 0.9×10^{-3} X_0

Drift Chamber geometry layout and material budget

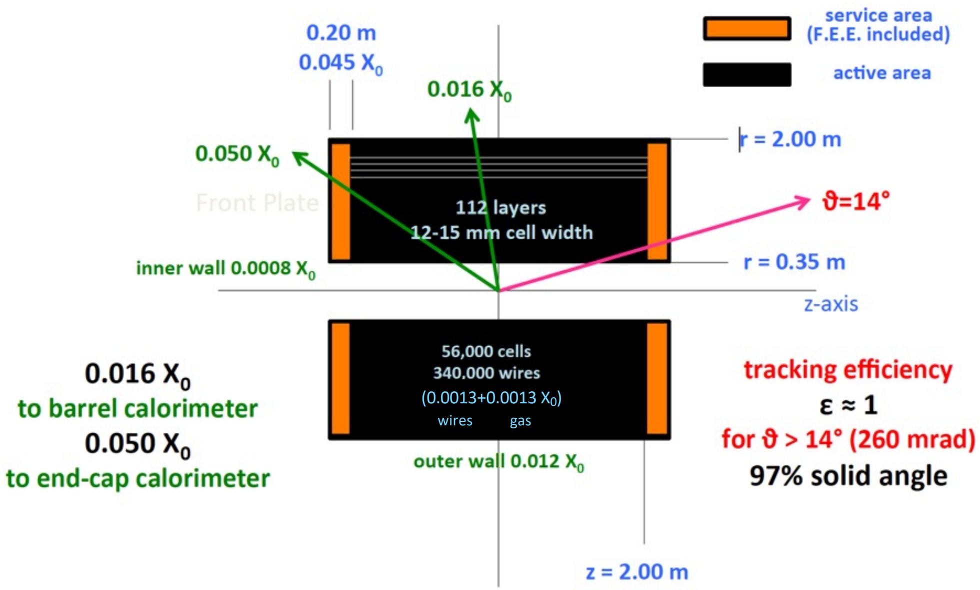

12 to 15 mm wide square cells, 5:1 field to sense wires ratio: 56,448 cells - 342,720 wires

14 co-axial super-layers, 8 layers each (112 total) with alternating sign stereo angles ranging from 50 to 250 mrad, in 24 equal azimuthal (15°) sectors

Material budget estimates

- Inner wall (from CMD3 drift chamber) — 8.4×10^{-4} X_0
  - 200 µm Carbon fiber
- Gas (from KLOE drift chamber) — 1.3×10^{-3} X_0
  - 90% He – 10% iC_4H_{10}
- Wires (from MEG2 drift chamber) — 1.3×10^{-3} X_0
  - 20 µm W sense wires 6.8×10^{-4} X_0
  - 40 µm Al field wires 4.3×10^{-4} X_0
  - 50 µm Al guard wires 1.6×10^{-4} X_0
- Outer wall (from Mu2e I-tracker studies) — 1.2×10^{-2} X_0
  - 2 cm composite sandwich (7.7 Tons)
- End-plates (from Mu2e I-tracker studies) — 4.5×10^{-2} X_0
  - wire cage + gas envelope
  - incl. services (electronics, cables,...)

Increase cell size to *w* > 1.5 cm (+10%)

(56,448 → 45,700 cells, 112 → 100 layers, 340,000 → 500,000 wires, 9 → 18 Ton)

and **replace 20 µm W and 40-50 µm Al** (5:1) with

(2 (0.5) µm Ag coated) **35 µm C wires** (10:1). Stability condition:

30 g < T_c < 87 g corresponding to ***270 (158) µm > δ_{grav} > 93 (54) µm***

(safety factor within ample margin!)

Contribution to m. scatt. from wires: 1.3×10^{-3} X_0 → 0.9×10^{-3} X_0

Wires: 1st challenge

Drift Chamber mechanical structure

Conceptual draft

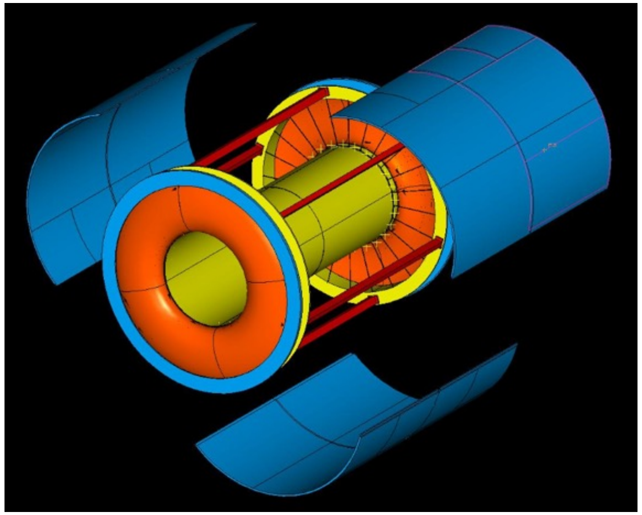

Separation of functions

Gas containment

Gas vessel can freely deform without affecting the internal wire position and mech. tension.

Wire support

Wire support structure not subject to differential pressure can be light and feed-through-less.

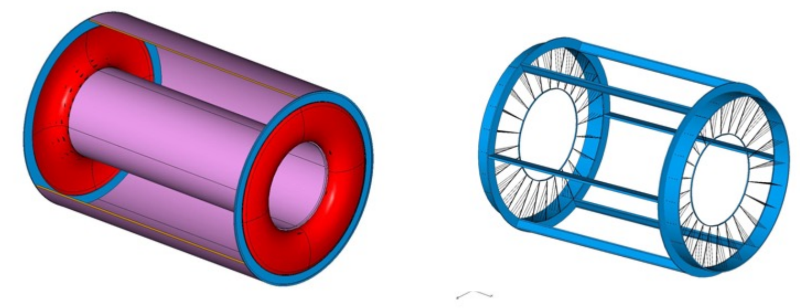

preliminary results from ANSYS (in progress)

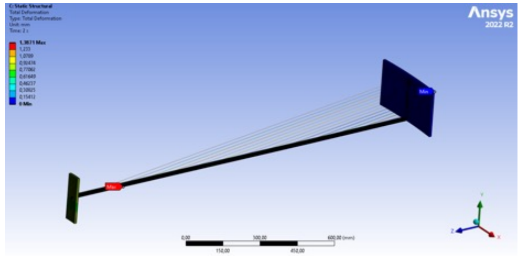

"traditional" drift chamber designs were based on the concept of anchoring the wires to a solid end plate, to sustain the load due to the wires tension (many Tons!). Result: **very massive end plates!**
"new concept" calls for separating the wire support, by counterbalancing the wire tension with external stays, like in a **cable-stayed bridge**, from the gas containment.

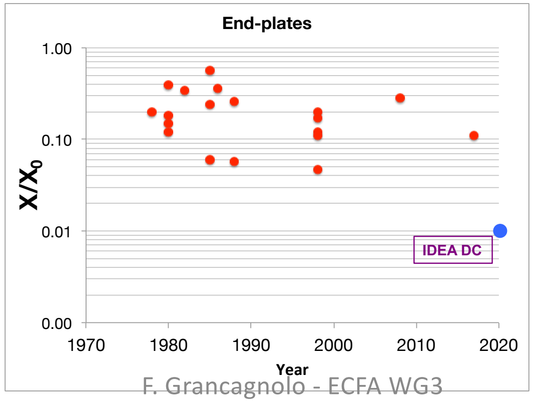

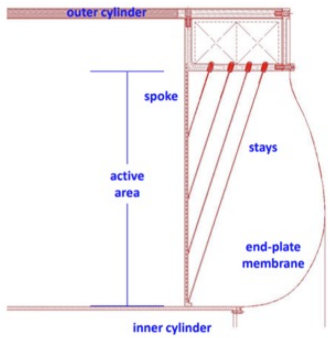

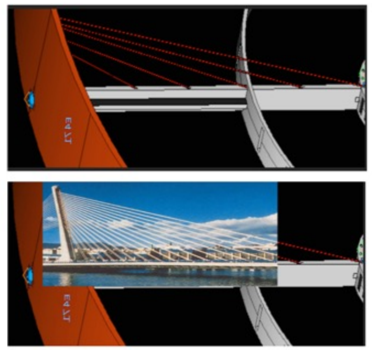

Drift Chamber mechanical structure

Conceptual draft

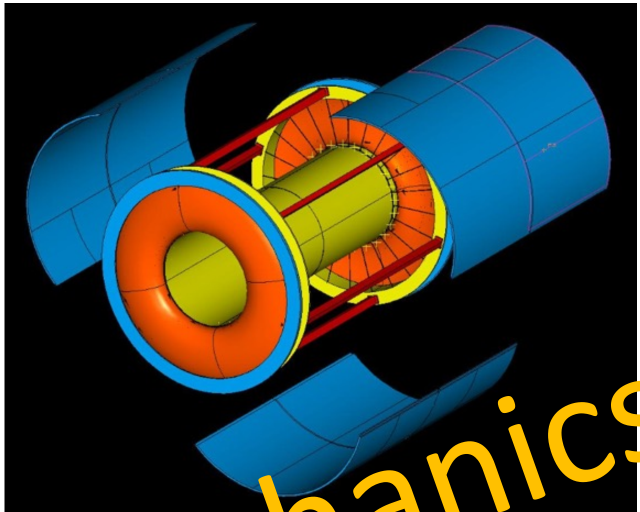

Separation of functions

Gas containment

Gas vessel can freely deform without affecting the internal wire position and mech. tension.

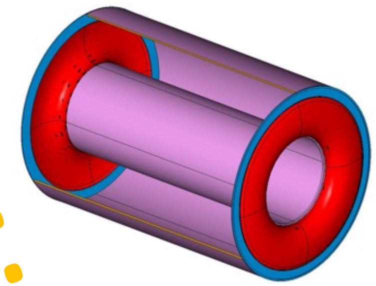

Wire support

Wire support structure not subject to differential pressure can be light and feed-through-less.

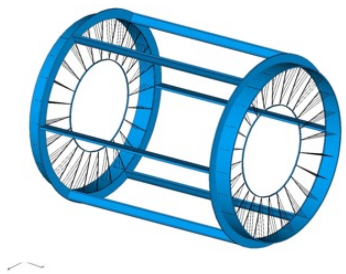

preliminary results from ANSYS
(in progress)

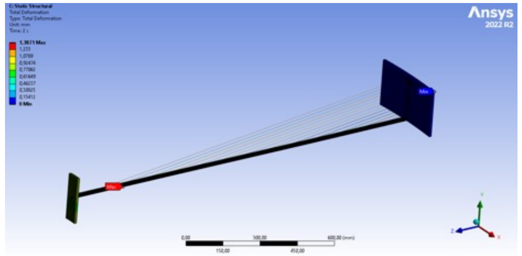

Mechanics: 2nd challenge

“traditional” drift chamber designs were based on the concept of anchoring the wires to a solid end plate, to sustain the load due to the wires tension (many Tons!). Result: **very massive end plates!**

“new concept” calls for separating the wire support, by counterbalancing the wire tension with external stays, like in a **cable-stayed bridge**, from the gas containment.

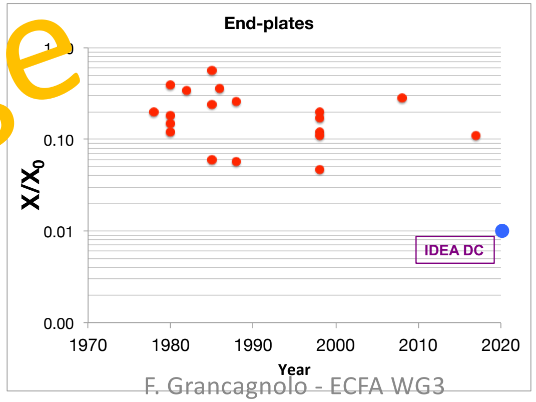

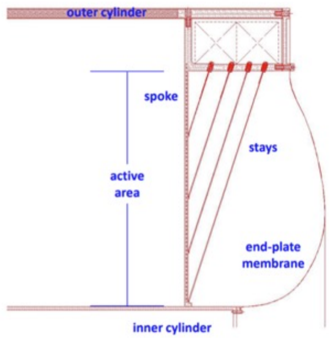

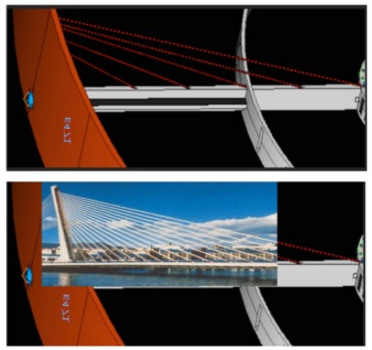

PID with dN_{cl}/dx in the time domain: simulations

2.0 m long tracks in 90/10 He/iC_4H_{10}

full simulation

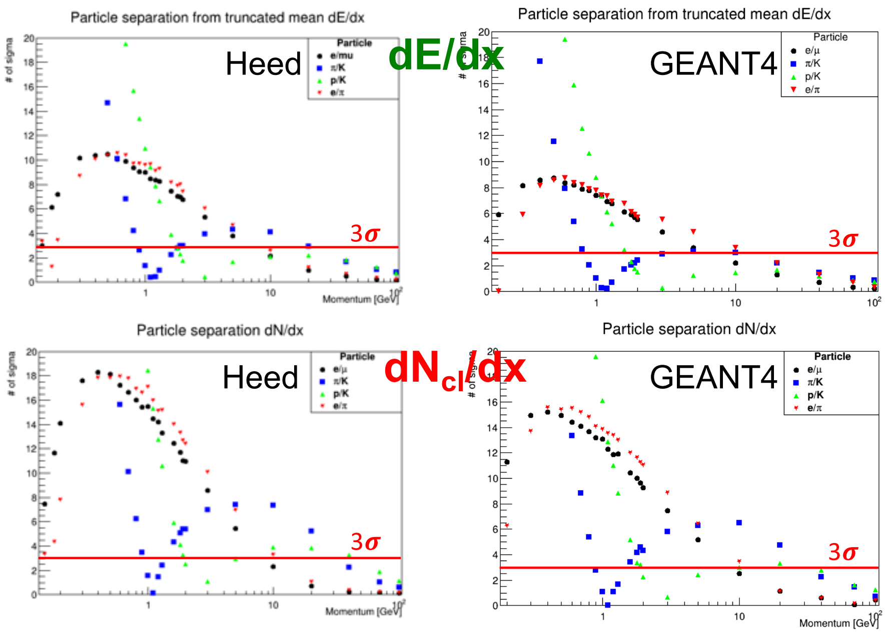

F. Cuna, N. De Filippis, F. Grancagnolo, G. Tassielli, Simulation of particle identification with the cluster counting technique, arXiv:2105.07064v1 [physics.ins-det] 14 May 2021

Geant4 uses the cluster density and the cluster size distributions derived from **Heed**, however, they **disagree**, most likely, due to a different choice of the E_{cut} parameter (the maximum energy of an electron still associated to a track in the simulation)

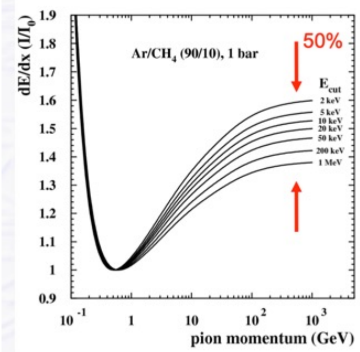

M. Hauschild Progress in dE/dx techniques used for particle identification NIM A379(1996) 436

IDEA drift chamber expected π/K separation

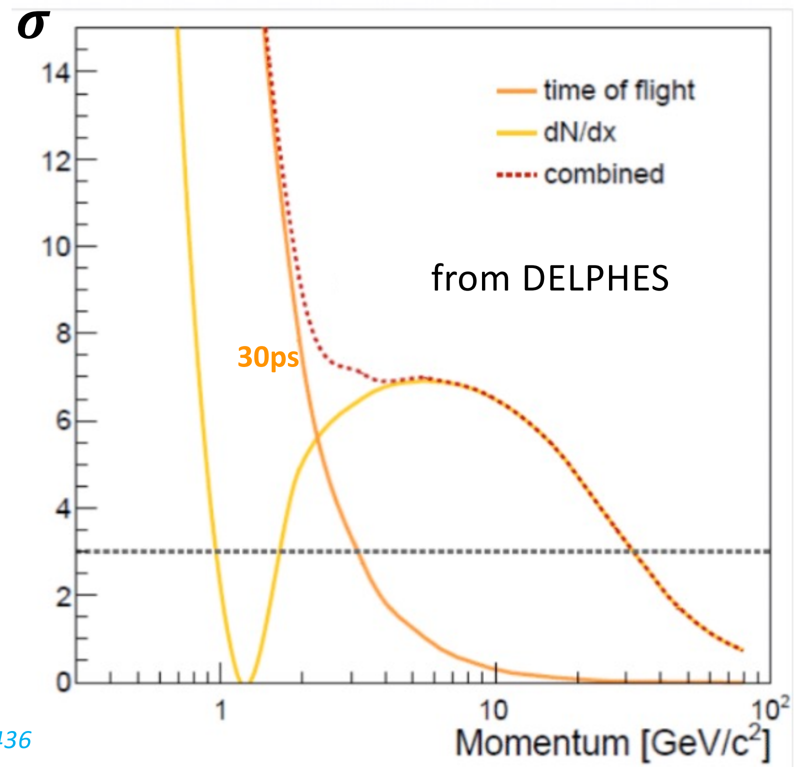

PID with dN_{cl}/dx in the time domain: simulations

2.0 m long tracks in 90/10 He/iC_4H_{10}

full simulation

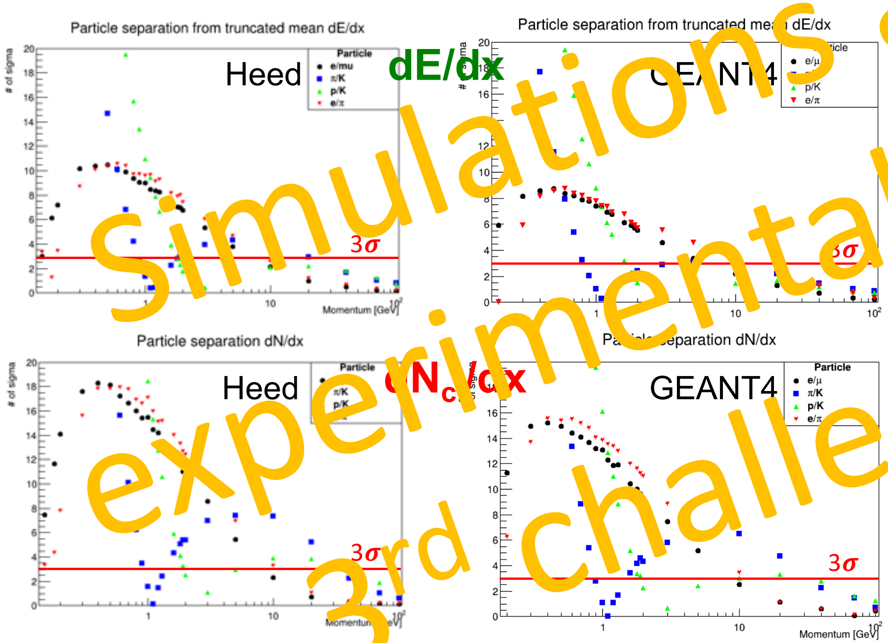

F. Cuna, N. De Filippis, F. Grancagnolo, G. Tassielli, *Simulation of particle identification with the cluster counting technique*, arXiv:2105.07064v1 [physics.ins-det] 14 May 2021

Simulations and experimental tests 3rd challenge

Geant4 uses the cluster density and the cluster size distributions derived from **Heed**, however, they **disagree**, most likely, due to a different choice of the **E_{cut}** parameter (the maximum energy of an electron still associated to a track in the simulation)

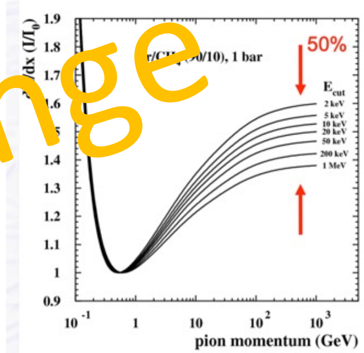

From: Michael Hauschild – *op. cit.*

IDEA drift chamber expected π/K separation

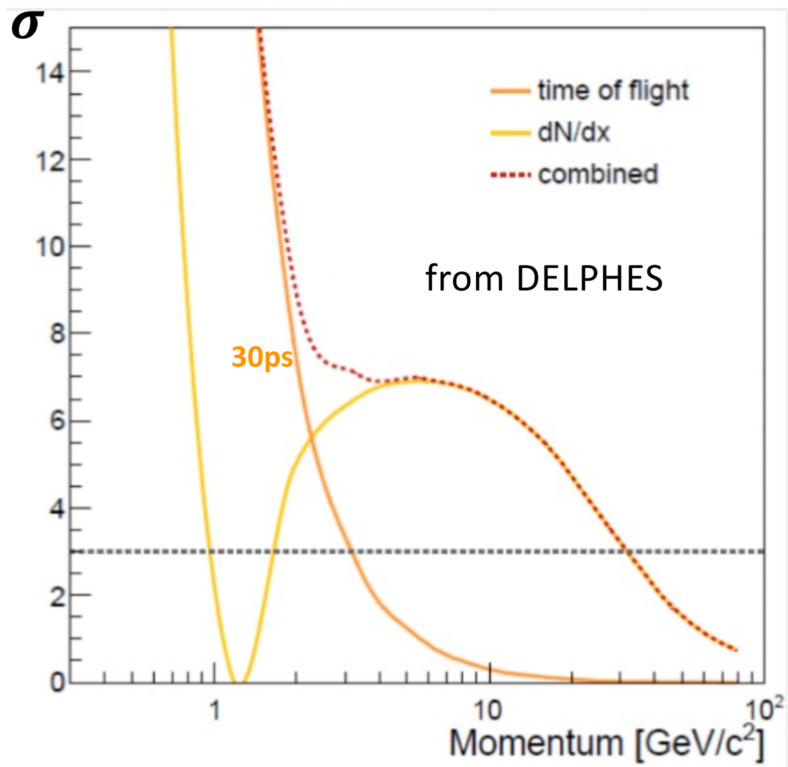

PID with dN_{cl}/dx in the time domain: requirements

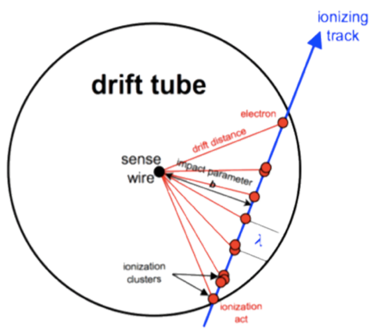

Determine, in the signal, the **ordered sequence of the electron arrival times**:

$$\{t_j^{el}\} \qquad j = 1, n_{el}$$

Based on the dependence of **the average time separation between consecutive clusters** and on the **time spread due to diffusion**, as a function of the drift time, **define** the **probability function**, that the ***j^th^*** **electron** belongs to the ***i^th^*** **cluster**:

$$P(j,i) \qquad j = 1, n_{el}, \quad i = 1, n_{cl}$$

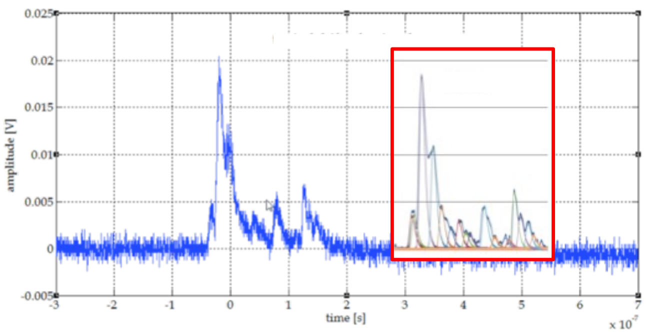

from this **derive** the most probable **time ordered sequence of the original ionization clusters**:

$$\{t_i^{cl}\} \qquad i = 1, n_{cl}$$

and the total number of clusters

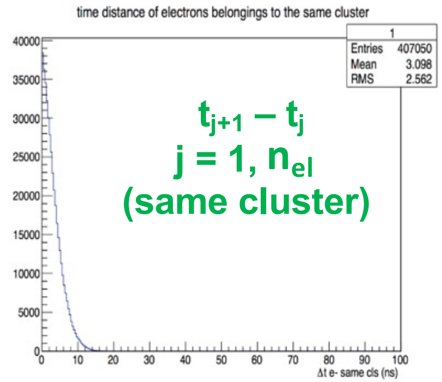

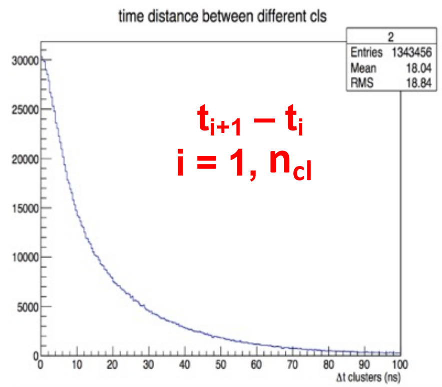

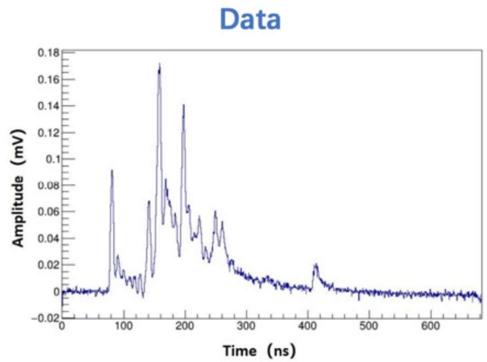

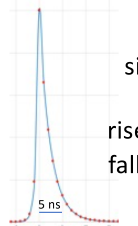

single electron simulation:
rise time ≲ 0.5 ns
fall time ~ 2.0 ns

Requirements

fast front-end electronics
(**bandwidth ~ 1 GHz**)
high sampling rate digitization
(**~ 2 GSa/s, 12 bits, >3 KB**)

PID with dN_{cl}/dx in the time domain: measurements

IDEA test prototypes (square drift tubes)

- Beam test at CERN-H8 during 2021 and 2022 with Fermi plateau muons (next beam test at CERN-T10 on muons relativistic rise, next month
- Simulations trained on data
- Peak finding algorithms trained on simulations

Derivative method

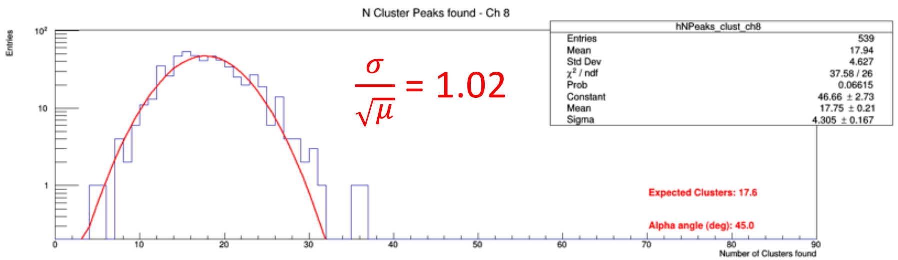

$$\frac{\sigma}{\sqrt{\mu}} = 1.02$$

Running template method

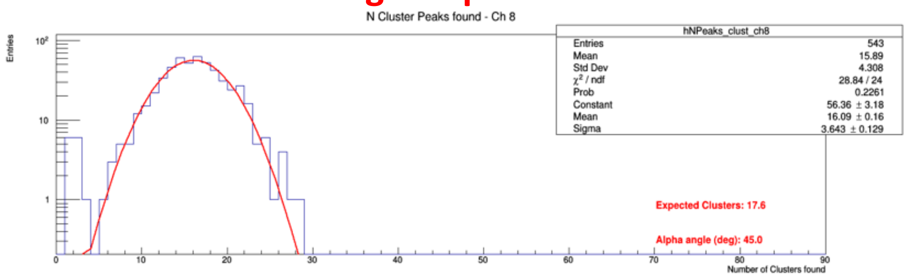

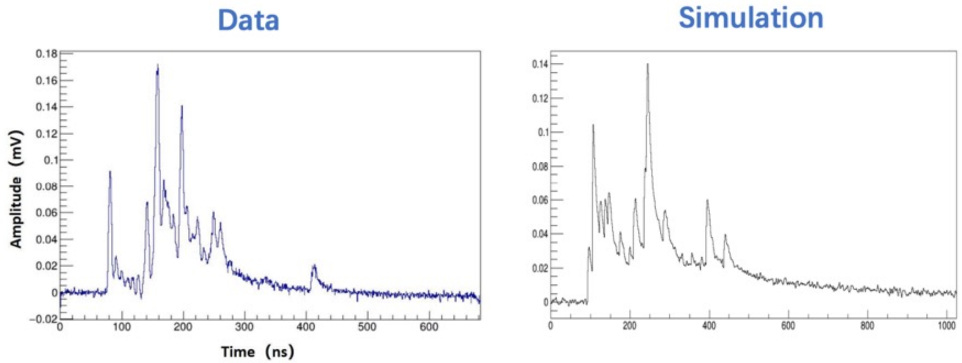

Machine Learning

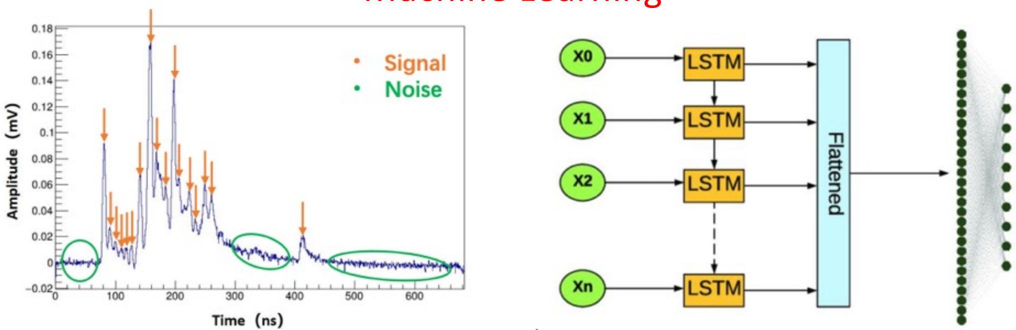

From Guang Zhao - IHEP

PID with dN_{cl}/dx in the time domain: measurements

IDEA test prototypes (square drift tubes)

- Beam test at CERN-H8 during 2021 and 2022 with Fermi plateau muons (next beam test at CERN-T10 on muons relativistic rise, next month
- Simulations trained on data
- Peak finding algorithms trained on simulations

Derivative method

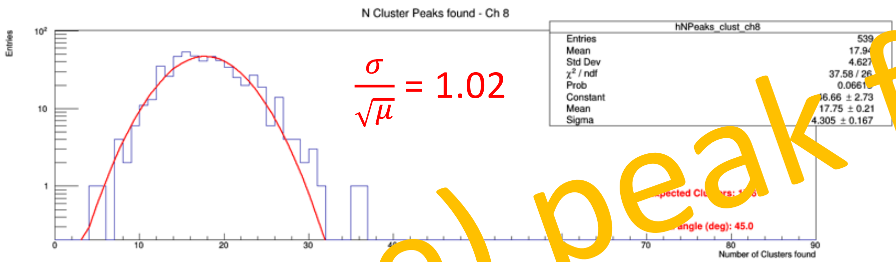

$\frac{\sigma}{\sqrt{\mu}} = 1.02$

Running template method

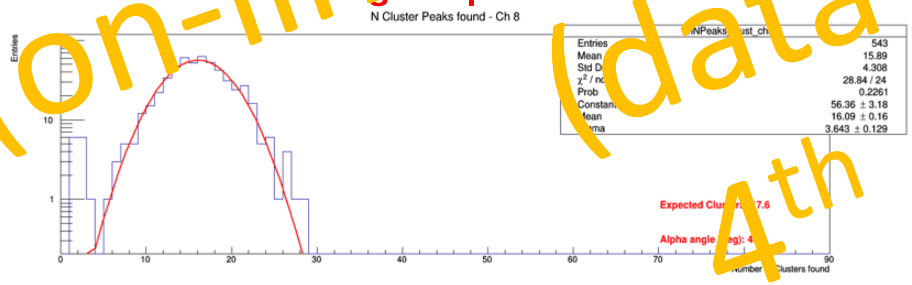

Data

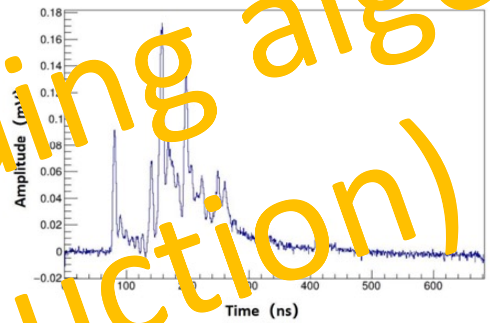

Simulation

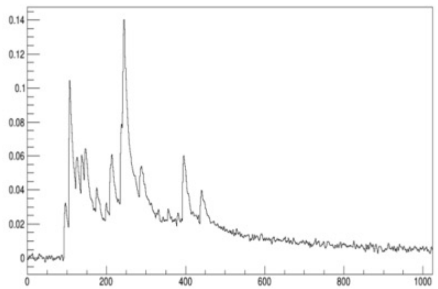

Machine Learning

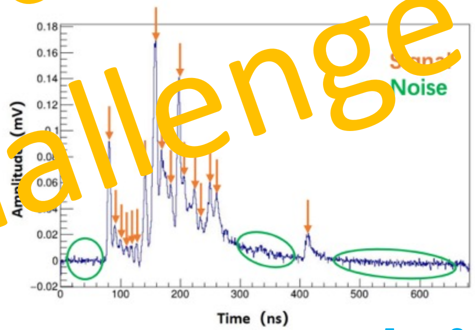

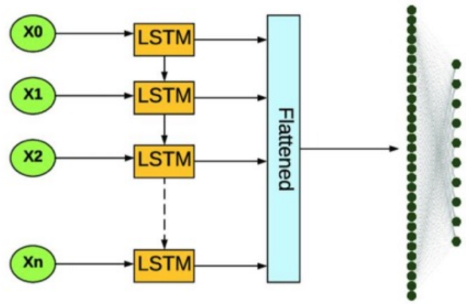

From Guang Zhao - IHEP

(on-line) peak finding algorithms
(data reduction)
4th challenge

Cluster Counting/Timing: fringe benefits

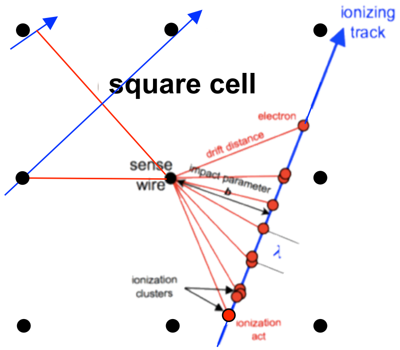

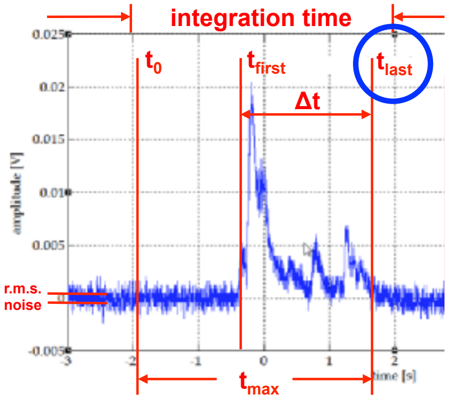

Given $\{t_i^{cl}\}$ $i = 1, n_{cl}$, by using statistical tools (**MPS**) or **ML techniques**, one can determine, hit by hit, the most probable **impact parameter**, thus reducing the **bias** and improving the average **spatial resolution** with respect to the one obtainable with the first cluster method alone.

Spatial resolution is expected to improve to **≲ 80 µm** (averaged over the whole cell)

Δt depends on impact parameter **b(t_{first})**

t_{max} (maximum drift time) ∽ **constant**

t_{last} defines the **trigger time: $t_0 = t_{last} - t_{max}$**

independently of b and track angle

t_{last} for 100 hits tracks **σ(t_{last}) ≈ 5 ns (r.m.s./√100)**

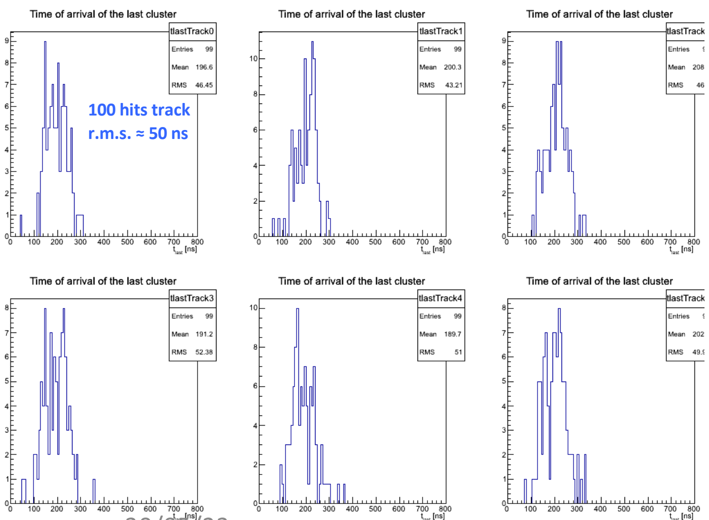

σ(t_0) as a function of N_{tracks} ($t_0 = t_{last} - t_{max}$)

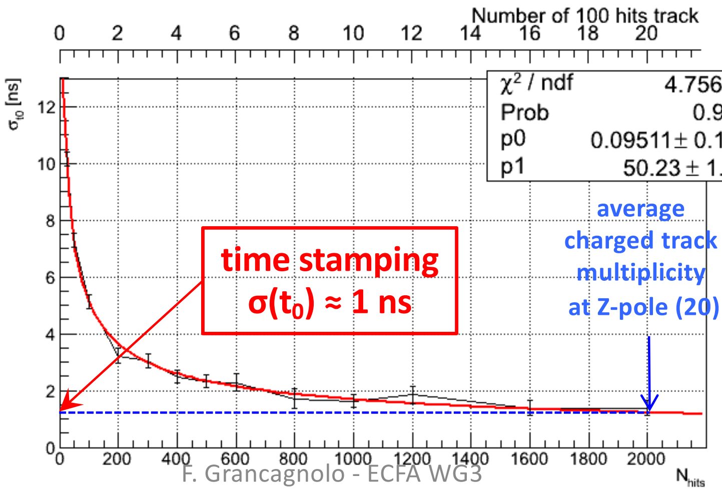

Longitudinal coordinate

charge division and time delay applied to individual clusters

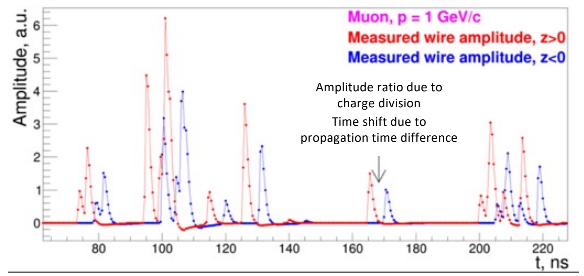

IDEA Drift Chamber Performance: full simulation

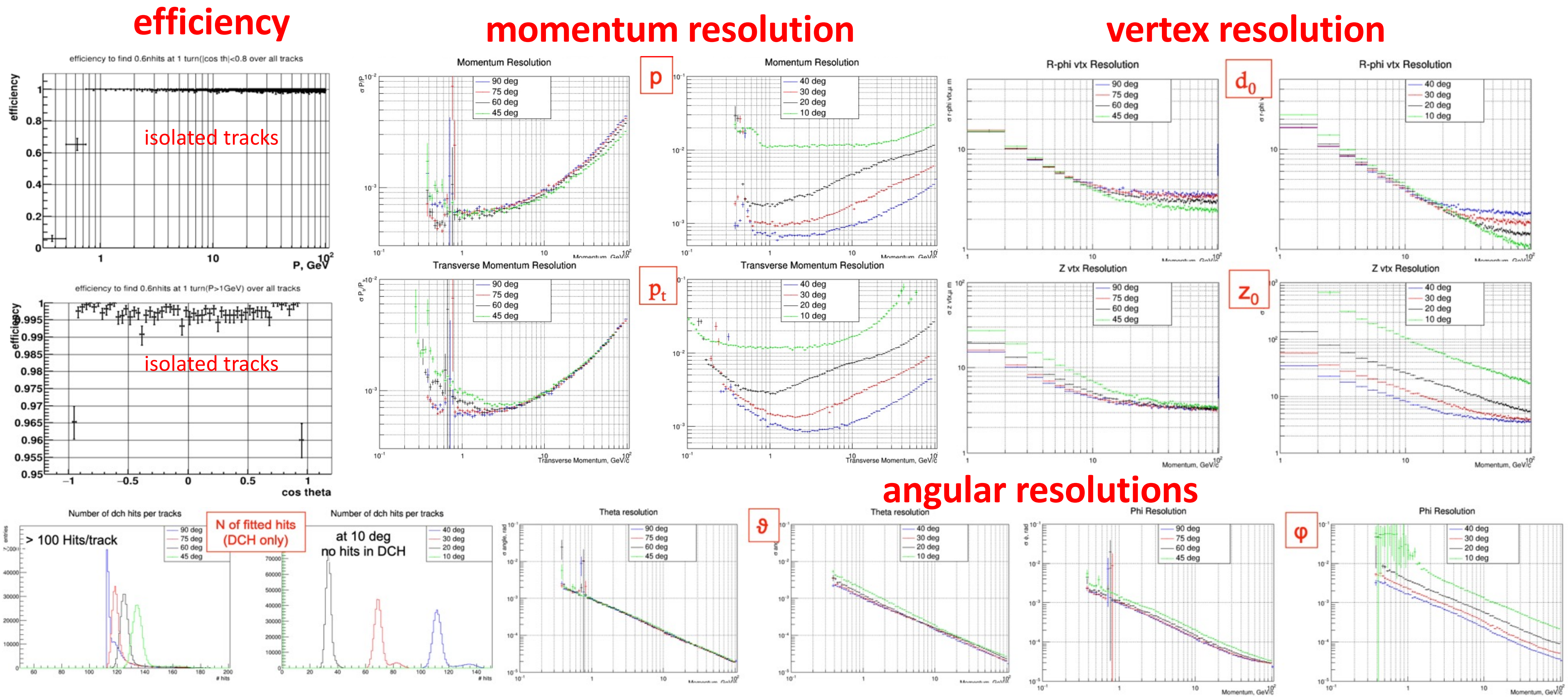

1st CHALLENGE: wire types – Carbon wires

SPECIALTY MATERIALS, INC.
Manufacturers of Boron and SCS Silicon Carbide Fibers and Boron Nanopowder
CARBON MONOFILAMENT

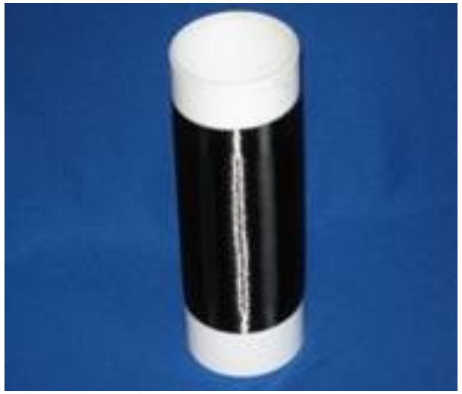

TYPICAL PROPERTIES

Diameter:	0.00136 +/- 0.0001" (34.5 +/- 2.5 μm)
Tensile Strength:	125 ksi (0.86 GPa) **0.65 GPa**
Tensile Modulus:	6 msi (41.5 GPa)
Electrical Resistivity:	3.6 x 10^{-3} ohm cm **37 KΩ/m**
Density:	1.8 g/cc

Specialty Materials, Inc.
1449 Middlesex Street
Lowell, Massachusetts 01851

Phone: 978-322-1900
Fax: 978-322-1970

CARBON MONOFILAMENT PRODUCT PRICE LIST
Effective October 1, 2017

Product	Quantity	Price LF
CARBON MONOFILAMENT	1 Million LF	$0.02
	500,000 LF	$0.03
	1,000 LF	$0.93

CARBON MONOFILAMENT PRODUCT PRICE LIST EFFECTIVE APRIL 1, 2019

Product	Quantity	Price per LF
CARBON MONOFILAMENT	1 Million LF	$0.02 **6 €/Km**
	500,000 LF	$0.03
	1,000 LF	$0.94

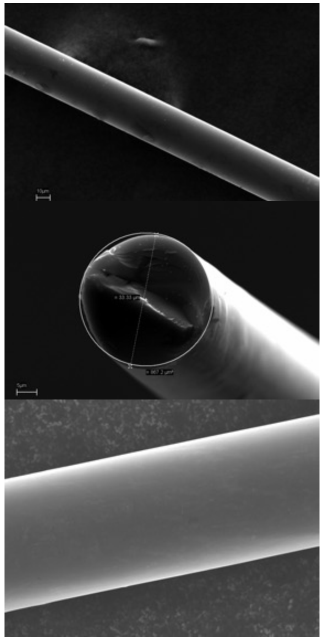

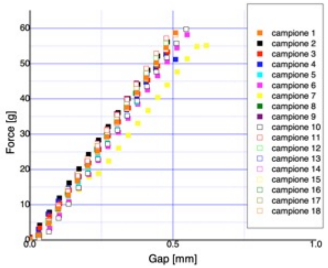

Metal coating by HiPIMS: High-power impulse magnetron sputtering

physical vapor deposition (PVD) of thin films based on magnetron sputter deposition (extremely high power densities of the order of kW/cm² in short pulses of tens of microseconds at low duty cycle <10%)

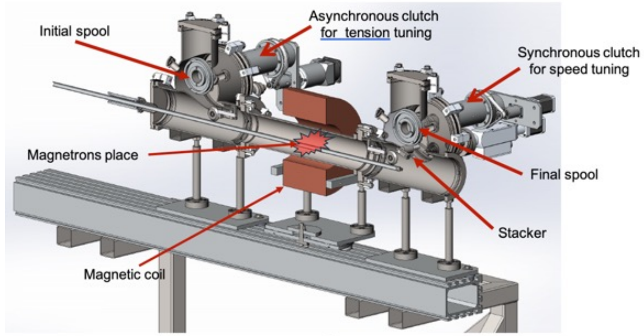

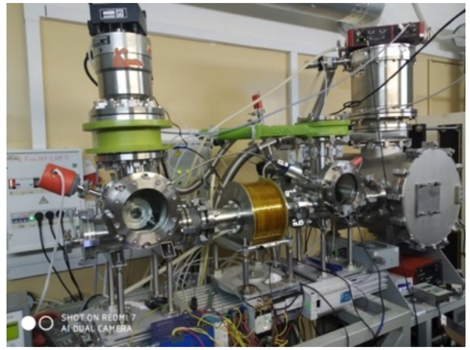

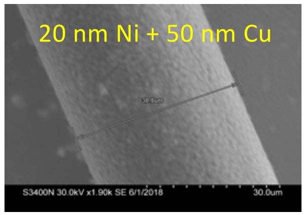

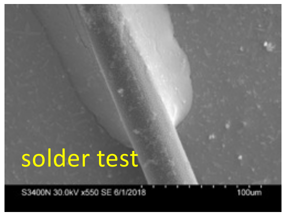

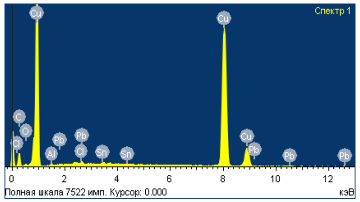

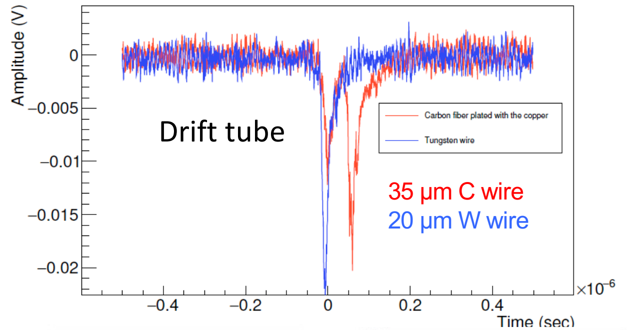

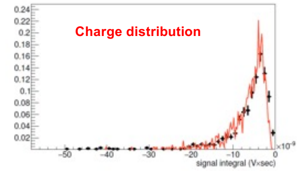

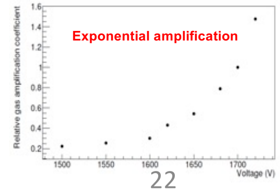

1st CHALLENGE: wire types – Carbon wires

Blue Sky R&D at in2p3 to find new wire material

3 groups implied
2 with wiring
machines

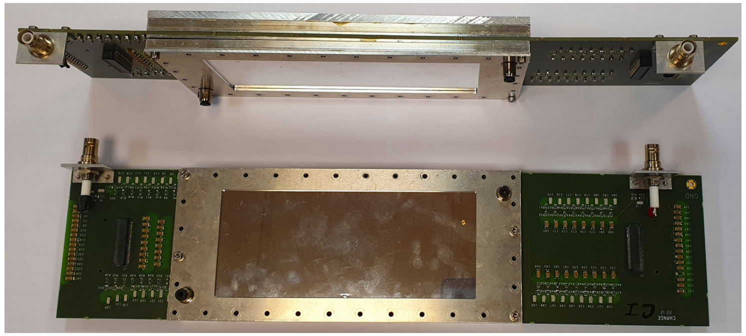

Design a simple detector (active area 17x7 cm^2) to test different types of wires

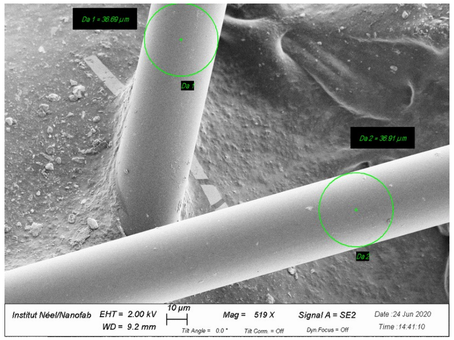

Carbone wires seen from SEM

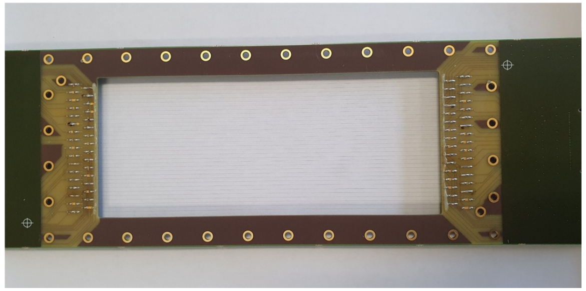

Carbon wire chamber soldered then glued

First results in 2017 *Carbon wire chamber at sub-atmospheric pressure, G. Charles et al., NIM A*

Tests with radioactive sources at 1 atm are on going for carbon wires and soldered AlMg5 wires.

Next step will be beam tests and **internationalize the collaboration**.

2^{nd} CHALLENGE: 350,000 wires!: wiring strategy

Evolution of the MEG2 drift chamber wiring

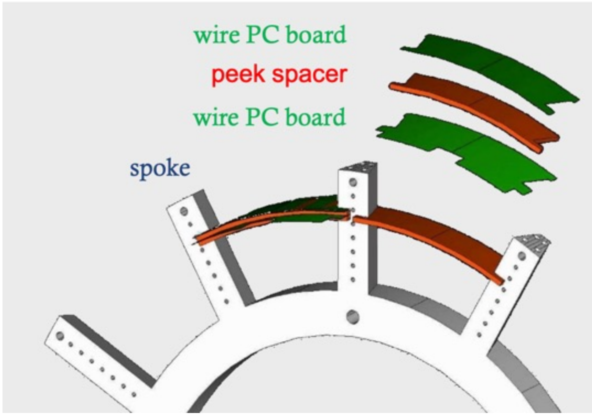

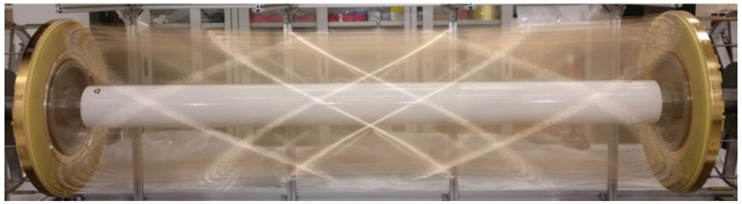

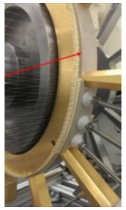

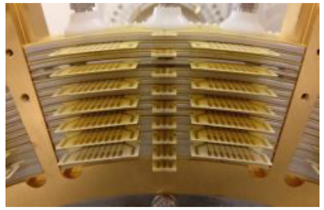

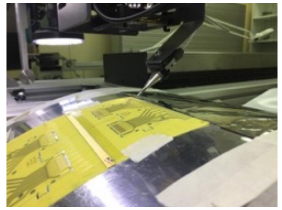

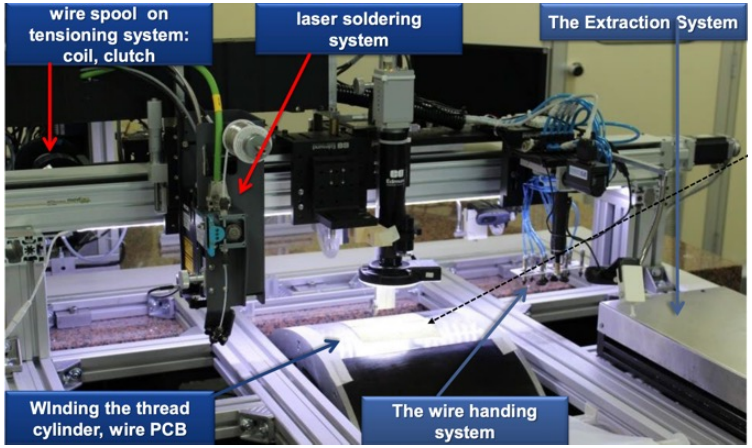

Wiring robot at INFN Lecce:
32 wires at once

MEG2: 12 wires/cm^2
IDEA: 4 wires/cm^2

Very different dimensions!
+ tension recovery scheme

2nd CHALLENGE: mechanics and materials

Conceptual design under development

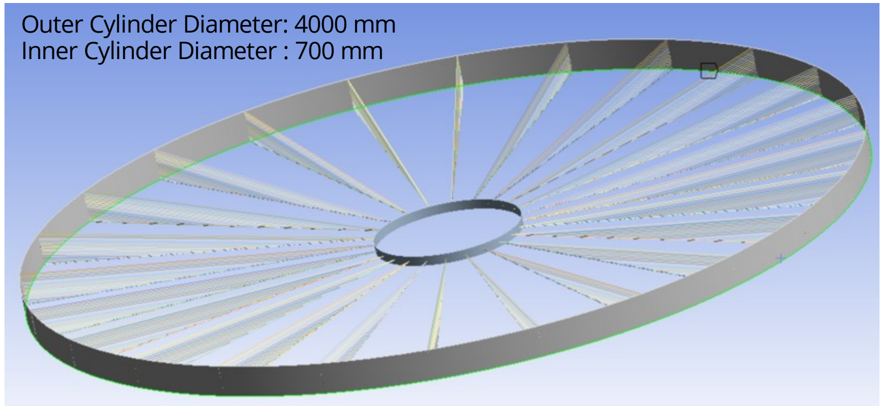

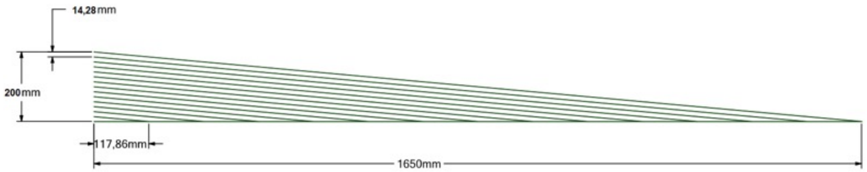

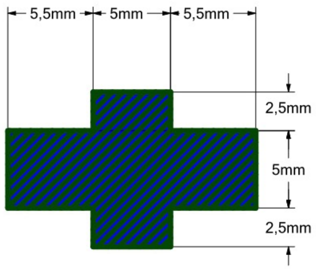

Cable/Stays: 3 mm dia.
(14 connected to each spoke)
Spokes: 16 x 10 mm (36)

spoke profile
unidirectional
C-fiber

Pre-stressed stays

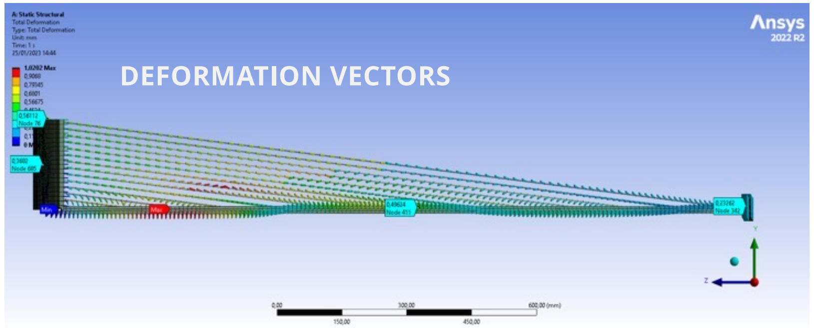

parameters optimization in progress

Test mockup (Al)

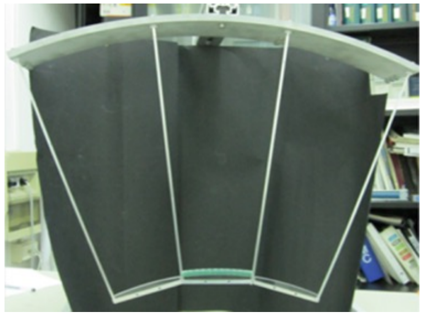

concept experimentally tested

stays tension recovery screws

Choice of gas envelope shape profile and materials soon to be addressed

3rd CHALLENGE: simulation – experimental tests

GEANT4 with **HEED** clusterization model

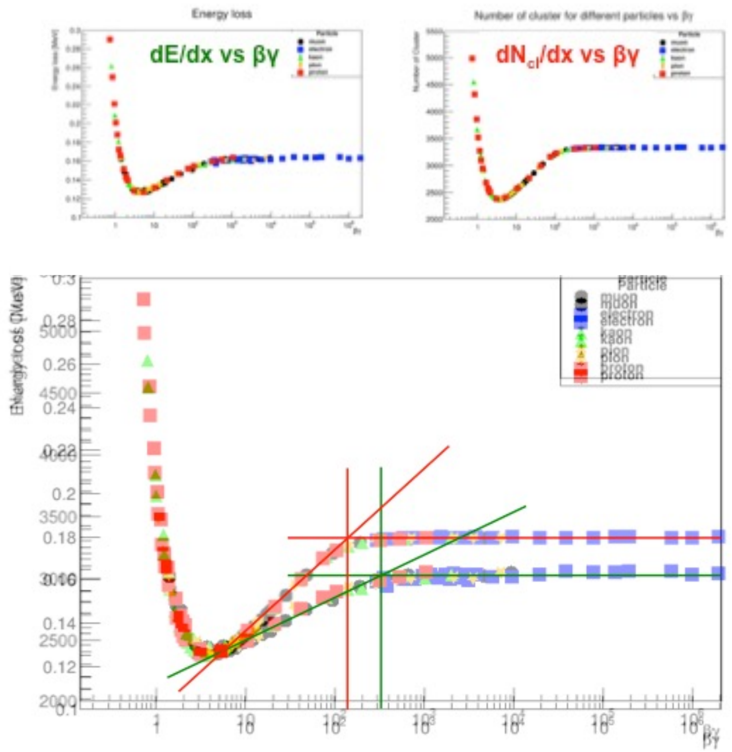

F. Cuna, N. De Filippis, F. Grancagnolo, G. Tassielli, Simulation of particle identification with the cluster counting technique, arXiv:2105.07064v1 [physics.ins-det] 14 May 2021

Higher values of Fermi plateau for **dN$_{cl}$/dx** w.r.t. **dE/dx**, yet reached at lower $\beta\gamma$ values and with a steeper slope

due to a choice of **E$_{cut}$** (the maximum energy of an electron still associated to a track in the simulation) parameter?

⇩

Experimental beam test campaign needed

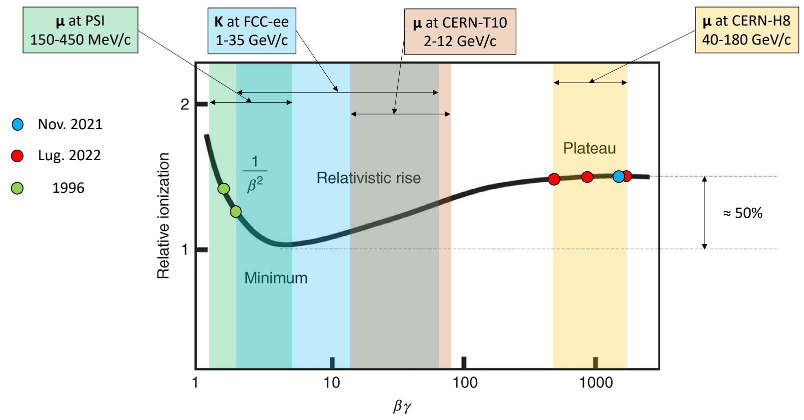

Next beam test
21 June – 4 July
at CERN-T10
with muons
2-12 GeV/c

4th CHALLENGE: peak finding algorithms

Simulation package (IHEP-Beijing contribution)

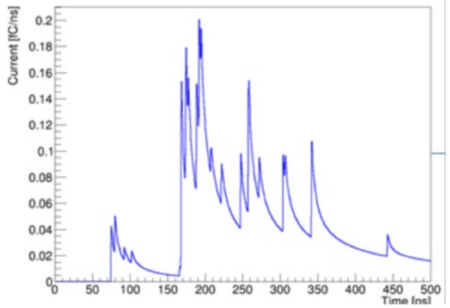

from GARFIELD++

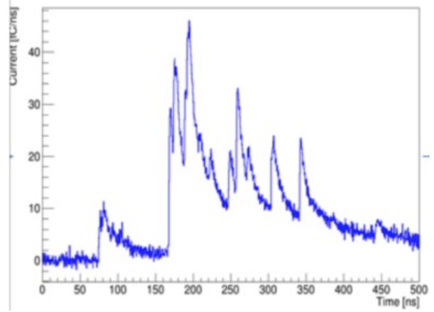

noise and pre-amp from data

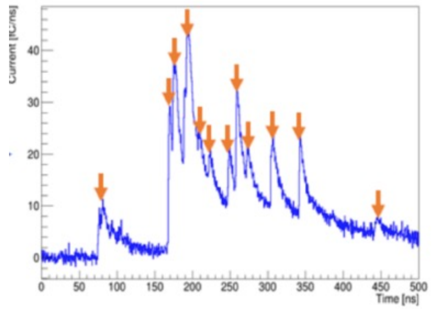

(derivative) reconstruction algorithm

Peak reconstruction efficiency: eff = #reco peaks/ #truth peaks = 82%.

Cluster reconstruction efficiency: eff = #reco cls/ #truth cls = 92.5%,

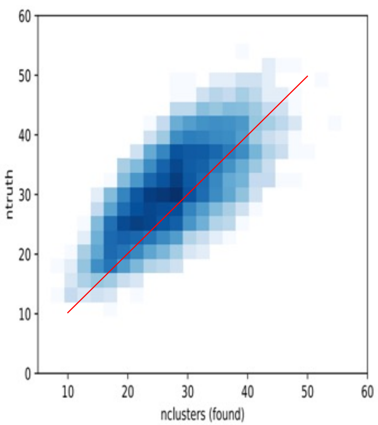

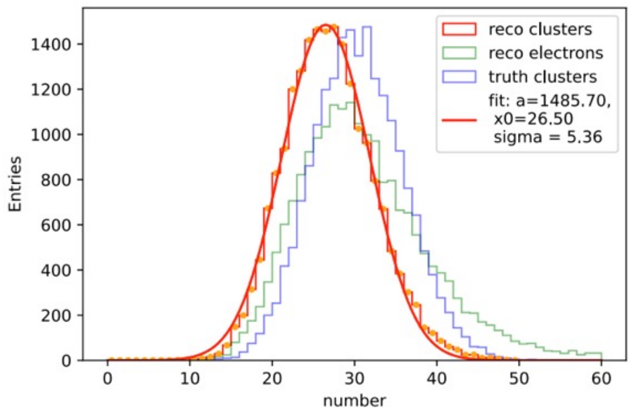

Alternative algorithms

Lecce derivative

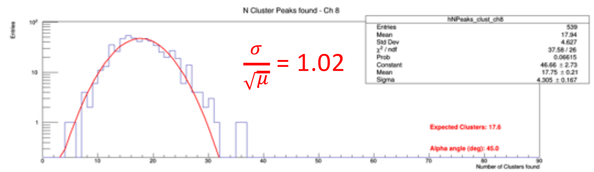

Lecce Running Template

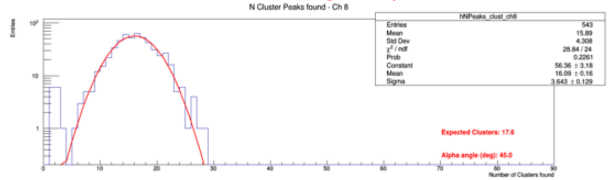

IHEP Machine Learning (RNN + CNN)

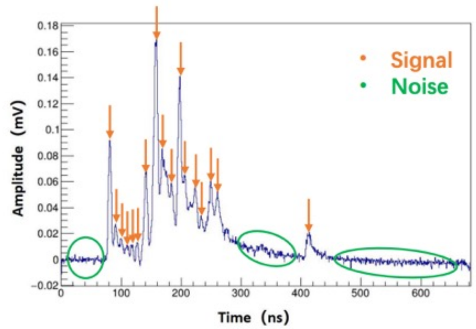

From Guang Zhao - IHEP

4th CHALLENGE: data reduction

The excellent performance of the **cluster finding** algorithms in offline analysis, relies on the assumption of being able to transfer the full spectrum of the digitized drift signals.
However …

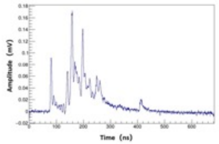

according to the **IDEA drift chamber operating conditions**:

- 56448 drift cells in 112 layers (~130 hits/track)
- maximum drift time of 500 ns
- cluster density of 20 clusters/cm
- signal digitization 12 bits at 2 Gsa/s

… and to the **FCC-ee running conditions at the Z-pole**

- 100 KHz of Z decays with 20 charged tracks/event multiplicity
- 30 KHz of $\gamma\gamma \longrightarrow$ hadrons with10 charged tracks/event multiplicity
- 2.5% occupancy due to beam noise
- 2.5% occupancy due to hits with isolated peaks

Reading both ends of the wires, ⇨ data rate ≥ 1 TB/s !

Solution consists in transferring, for each hit drift cell, instead of the full signal spectrum, only the minimal information relevant to the application of the **cluster timing/counting techniques**, i.e.:

the amplitude and **the arrival time** of each peak
associated with each individual ionisation electron.

This can be accomplished by using a **FPGA** for the **real time analysis** of the data generated by the drift chamber and successively digitized by an ADC.

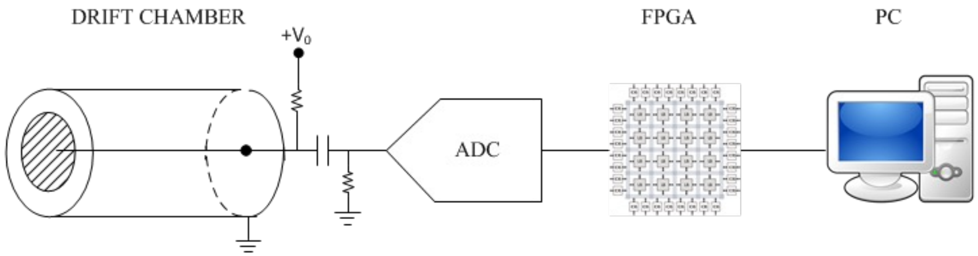

Single channel solution has been successfully verified.
G. Chiarello et al., The Use of FPGA in Drift Chambers for High Energy Physics Experiments May 31, 2017
DOI: 10.5772/66853

With this procedure **data transfer rate is reduced to ~ 25 GB/s**
Extension to a 4-channel board is in progress. Ultimate goal is a multi-ch. board (128 or 256 channels) to **reduce cost** and complexity of the system and to gain flexibility in determining the **proximity correlations** between hit cells for track **segment finding** and for **triggering** purposes.

Implementing ML algorithms on FPGA for peak finding

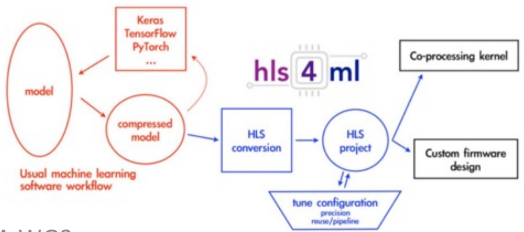

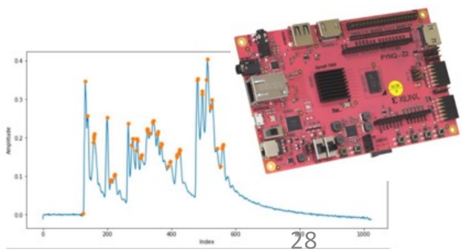

CONCLUSIONS